



## Supporting Information

for *Adv. Sci.*, DOI 10.1002/advs.202105787

### Uncovering a Vital Band Gap Mechanism of Pnictides

*Jindong Chen, Qingchen Wu, Haotian Tian, Xiaotian Jiang, Feng Xu, Xin Zhao, Zheshuai Lin, Min Luo\* and Ning Ye\**

Supporting Information  
© 2022 Wiley-VCH GmbH  
69451 Weinheim, Germany

## Uncovering a Vital Band Gap Mechanism of Pnictides

Jindong Chen,<sup>[a], [e]</sup> Qingchen Wu,<sup>[c]</sup> Haotian Tian,<sup>[a]</sup> Xiaotian Jiang,<sup>[d]</sup> Feng Xu,<sup>[a]</sup> Xin Zhao,<sup>[a]</sup> Zheshuai Lin,<sup>[c]</sup> Min Luo<sup>[a]\*</sup> and Ning Ye<sup>[a], [b]\*</sup>

**Abstract:** Pnictides are superior IR NLO material candidates, but the exploration of NLO pnictides is still tardy due to lack of rational material design strategies. An in-depth understanding structure-performance relationship is urgent for designing novel and eminent pnictide NLO materials. Herein, we unraveled a vital band gap mechanism of pnictides, namely P atom with low coordination numbers (2 CN) will cause the decrease of band gap due to the delocalization of non-bonding electron pairs. Accordingly, a general design paradigm for NLO pnictides, ionicity–covalency–metallicity regulation was proposed for designing wide-band gap NLO pnictides with maintained SHG effect. Driven by this idea, millimeter-level crystals of MgSiP<sub>2</sub> were synthesized with a wide band gap (2.34 eV), a strong NLO performance (3.5 × AgGaS<sub>2</sub>) and a wide IR transparency range (0.53–10.3 μm). This work provides an essential guidance for the future design and synthesis of NLO pnictides, and also opens a new perspective at Zintl chemistry important for other material fields.

**Table of Contents****Table S1.** Crystallographic Data and Refinement Details for MgSiP<sub>2</sub>.

Formula	MgSiP <sub>2</sub>
Formula weight	114.34
Temperature/K	293
Radiation	Ga K <sub>a</sub> ( $\lambda = 1.34139$ )
Crystal system	tetragonal
Space group	I-42d
a/Å	5.7156(5)
c/Å	10.074(2)
$\alpha/^\circ$	90
$\beta/^\circ$	90
$\gamma/^\circ$	90
Volume/Å <sup>3</sup>	329.11(10)
Z	4
p calc (g/cm <sup>3</sup> )	2.308
$\mu$ (mm <sup>-1</sup> )	9.737
F (000)	224
Index ranges	-5 ≤ h ≤ 3, -7 ≤ k ≤ 6, -11 ≤ l ≤ 12
Reflections collected	395
Independent reflections	175 [ $R_{\text{int}} = 0.0141$ ]
Data/restraints/parameters	175/0/11
Goodness-of-fit on F <sup>2</sup>	1.212
Final R indexes [ $>= 2\sigma (I)$ ]	$R_1 = 0.0328$ , $wR_2 = 0.0862$
Final R indexes [all data]	$R_1 = 0.0330$ , $wR_2 = 0.0866$
Largest diff. peak/hole / e Å <sup>-3</sup>	0.596/-0.659
Flack parameter	0.1(5)

**Table S2.** The relationship between the coordination number of P atom and the band gap of phosphides.

Compounds	Coordination number of P atom (CN)	Band gap (eV)	Reference
Zn <sub>3</sub> PI <sub>3</sub>	4	2.85	1
Cd <sub>2</sub> PCl <sub>2</sub>	4	>2.5	2
Cd <sub>3</sub> PI <sub>3</sub>	4	2.44	1
GaP	4	2.4	3
MgSiP <sub>2</sub>	4	2.33	4
Cd <sub>4</sub> P <sub>2</sub> Cl <sub>3</sub>	4	2.36	5
CdSiP <sub>2</sub>	4	2.2	6
α-ZnP <sub>2</sub>	4	2.25	7
α-CdP <sub>2</sub>	4	2.0	8
IrSi <sub>3</sub> P <sub>3</sub>	4	1.93	9
RuSi <sub>4</sub> P <sub>4</sub>	4	1.83	9
NaGe <sub>3</sub> P <sub>3</sub>	3	2.06	10
SiP (monolayer)	3	2.59	11
Ba <sub>2</sub> Si <sub>3</sub> P <sub>6</sub>	2 and 3	1.88	12
KSi <sub>2</sub> P <sub>3</sub>	2 and 3	1.72	13
BaSi <sub>7</sub> P <sub>10</sub>	2 and 3	1.1	14
SrSi <sub>7</sub> P <sub>10</sub>	2 and 3	1.1	14
Ba <sub>2</sub> SiP <sub>4</sub>	2	1.45	15

$\text{Sr}_2\text{SiP}_4$	2	1.41	15
$\text{BaGe}_2\text{P}_2$	2	1.36	16
$\text{LaSiP}_3$	1, 2 and 3	1.3	17
$\beta\text{-Ca}_2\text{CdP}_2$	1, 2 and 3	1.55	18

**Table S3.** Calculated values of  $g_{ijk}$  and  $C$ .

Compounds	Groups	$g_{ijk}$	$C$
	[ZnP <sub>4</sub> ]	$g_{123} = 0.99950$	0.99949
ZnGeP <sub>2</sub>	[GeP <sub>4</sub> ]	$g_{123} = 0.99947$	
	[AgS <sub>4</sub> ]	$g_{123} = 0.98764$	0.98513
AgGaS <sub>2</sub>	[GaS <sub>4</sub> ]	$g_{123} = 0.98263$	
	[MgP <sub>4</sub> ]	$g_{123} = 0.98653$	0.98521
MgSiP <sub>2</sub>	[SiP <sub>4</sub> ]	$g_{123} = 0.98389$	

**Table S4.** Comparison of MgSiP<sub>2</sub> with famous and recently reported NLO chalcogenides.

Compounds	$E_g$ (eV)	$d_{ij}$ (pm/V)	Reference
MgSiP <sub>2</sub>	2.34	31.2	this work
AgGaS <sub>2</sub>	2.75	14	19
AgGaSe <sub>2</sub>	1.83	30	19
BaGa <sub>4</sub> Se <sub>7</sub>	2.64	20.6	20
LiInSe <sub>2</sub>	2.83	12.5	21
BaGa <sub>2</sub> GeSe <sub>6</sub>	2.31	23.6	19
AgGaGeS <sub>4</sub>	2.78	15	22
AgGaGe <sub>5</sub> Se <sub>12</sub>	2.2	29	23
CdSe	1.65	36	24
m-Ga <sub>2</sub> Se <sub>3</sub>	1.86	23.2	25
Sr <sub>6</sub> Cd <sub>2</sub> Sb <sub>6</sub> O <sub>7</sub> S <sub>10</sub>	1.89	27.8	26
SnI <sub>4</sub> ·(S <sub>8</sub> ) <sub>2</sub>	2.17	6.3	27
Na <sub>2</sub> CdSn <sub>2</sub> Se <sub>6</sub>	2.15	20.3	28
Ba <sub>6</sub> In <sub>6</sub> Zn <sub>4</sub> Se <sub>19</sub>	2.2	16.3	29
Hg <sub>2</sub> GeSe <sub>4</sub>	1.17	24.56	30

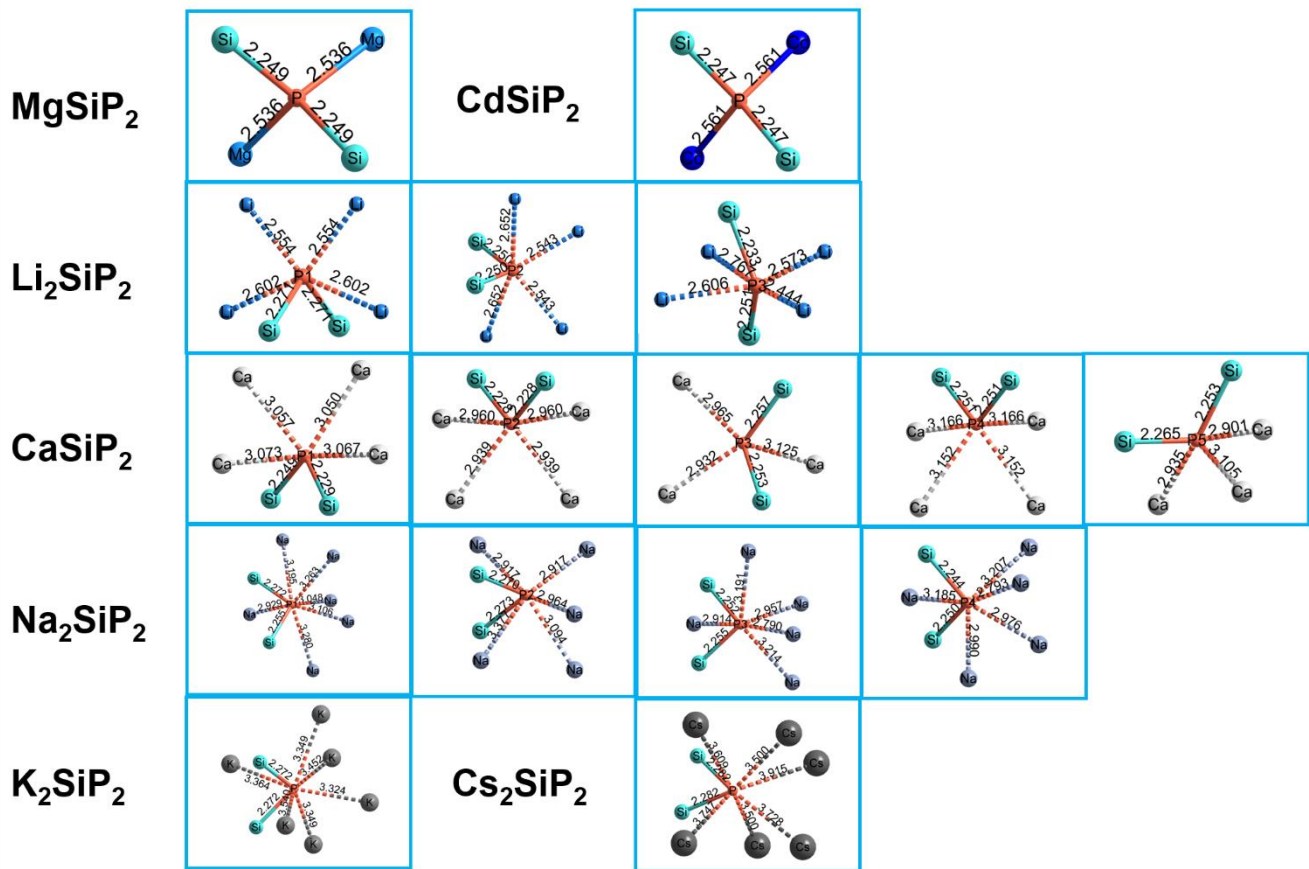


**Figure S1.** Coordination environment of P atoms.

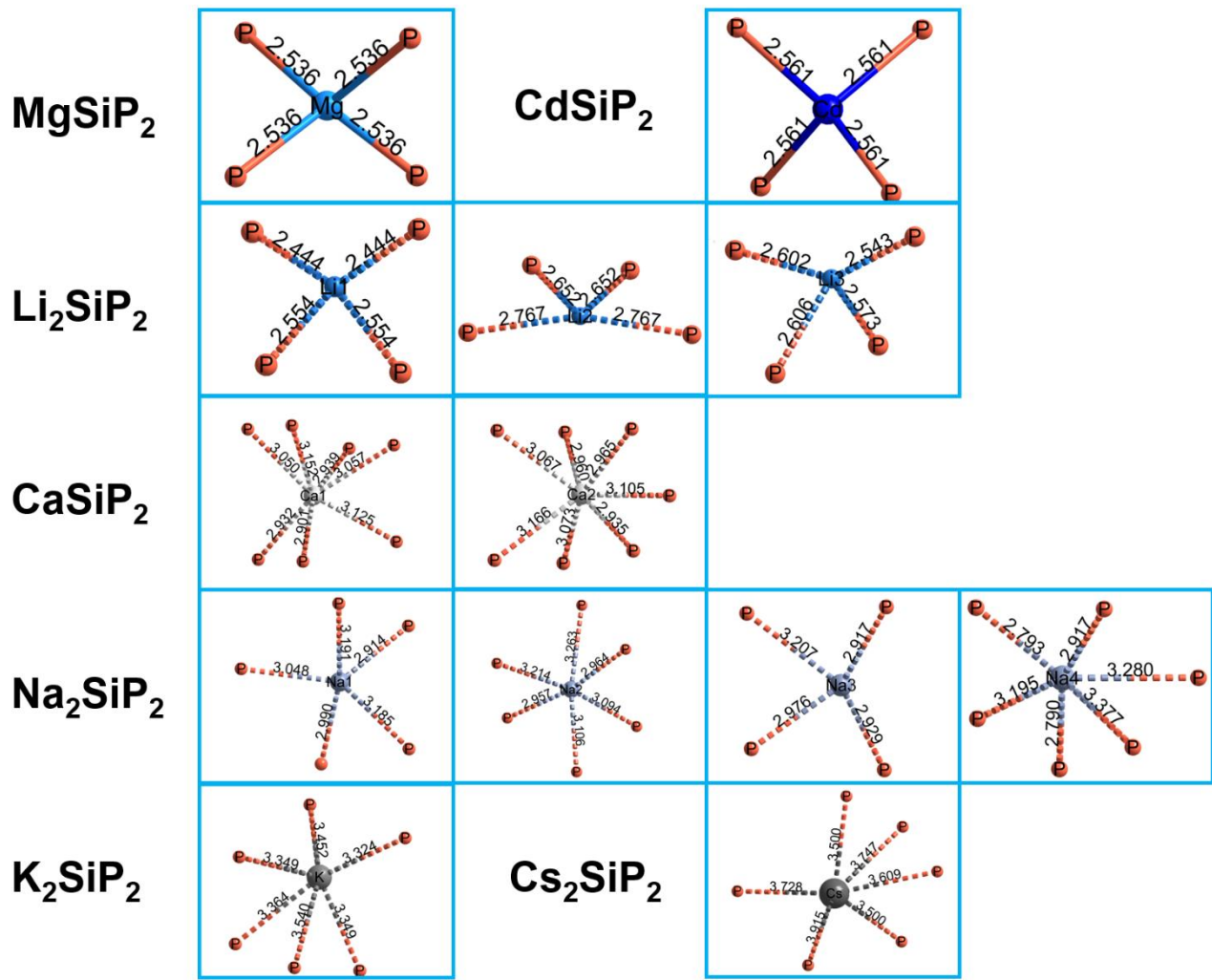
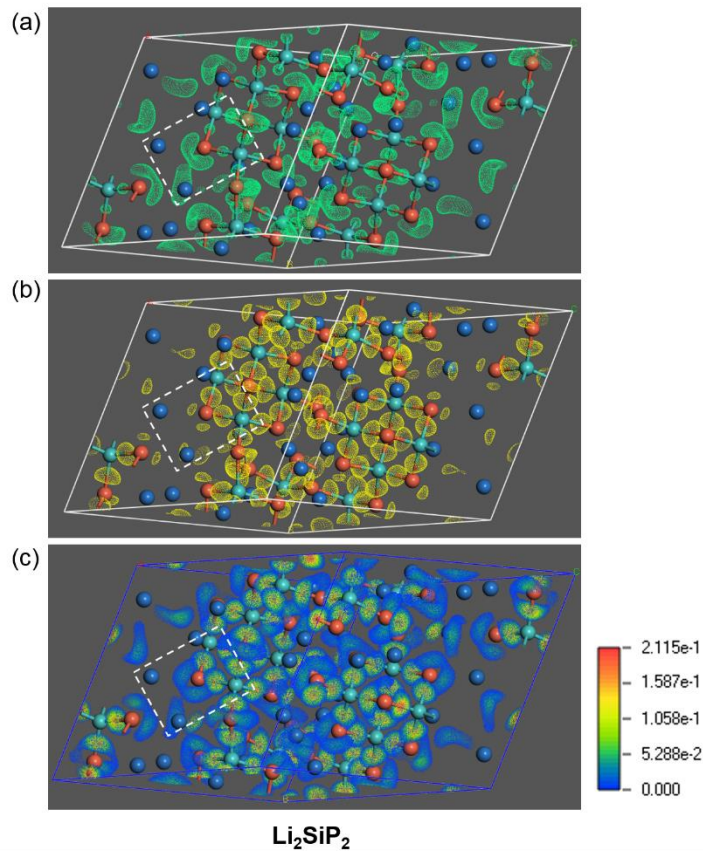
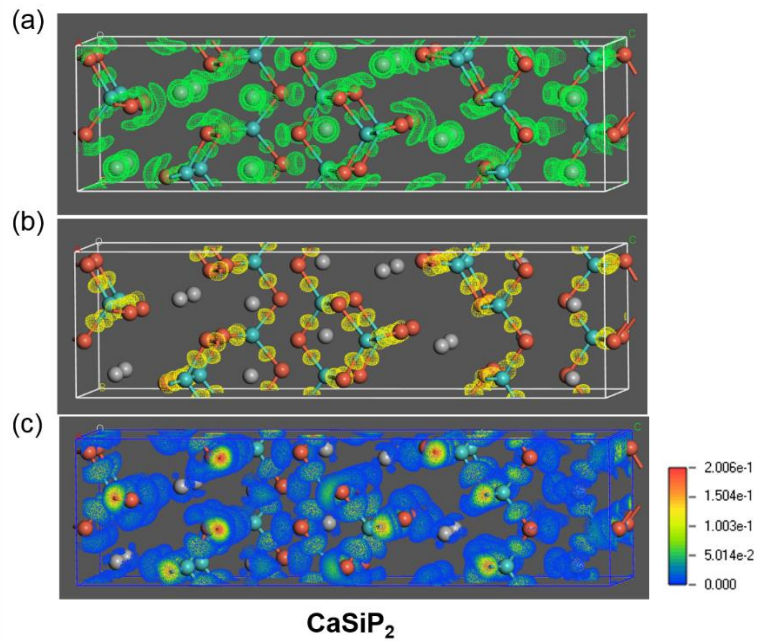


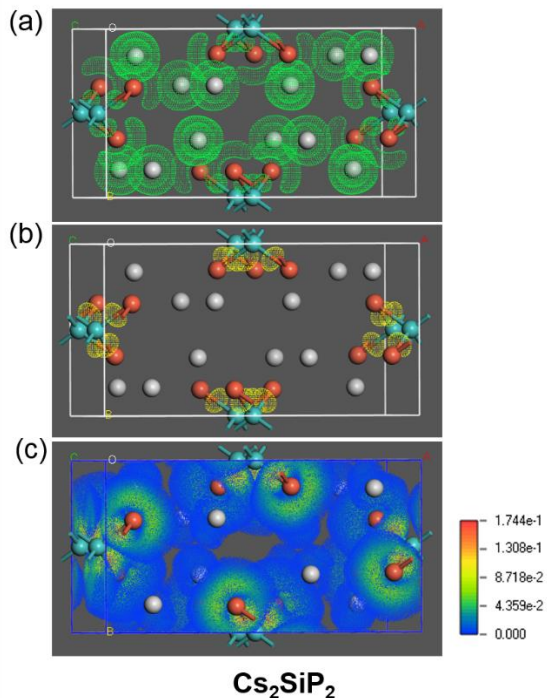
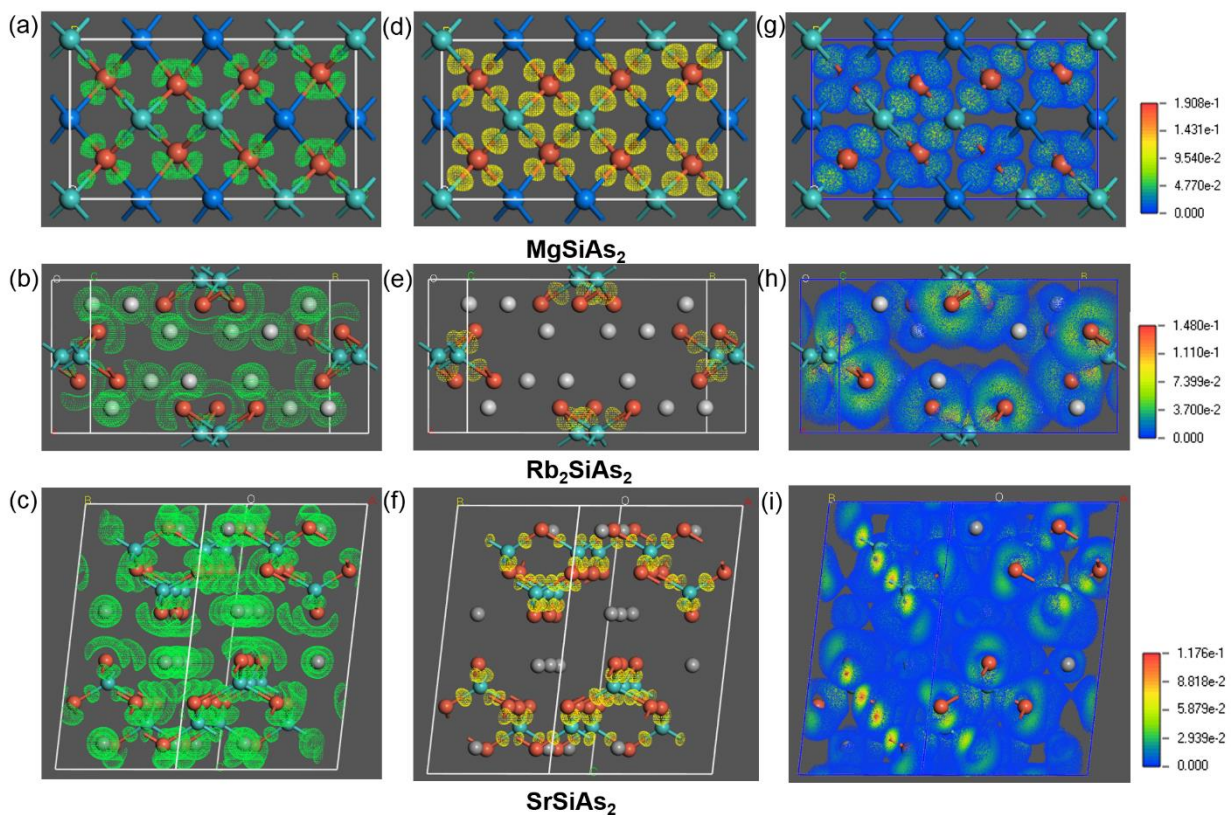
Figure S2. Coordination environment of A site atoms.

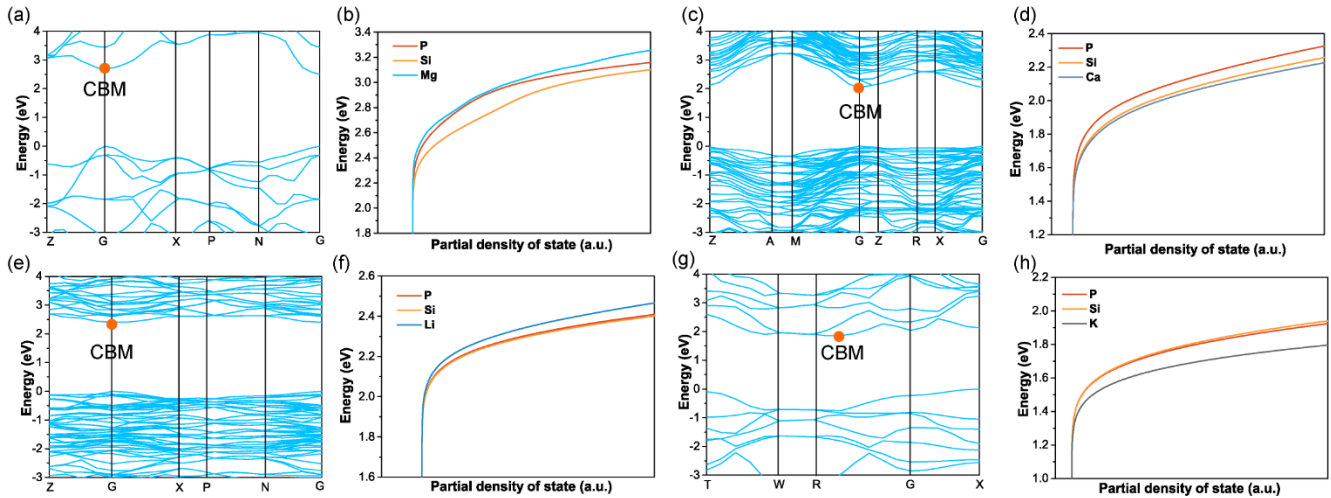


**Figure S3.** 3D ELF isosurfaces at  $\eta = 0.5$  (a), EDD isosurfaces at  $\eta = 1/2 \times \text{maximum}$  (b) and EDD distributions (c) of  $\text{Li}_2\text{SiP}_2$ . White dashed boxes represent two nearest Si and Li atoms of P atom.

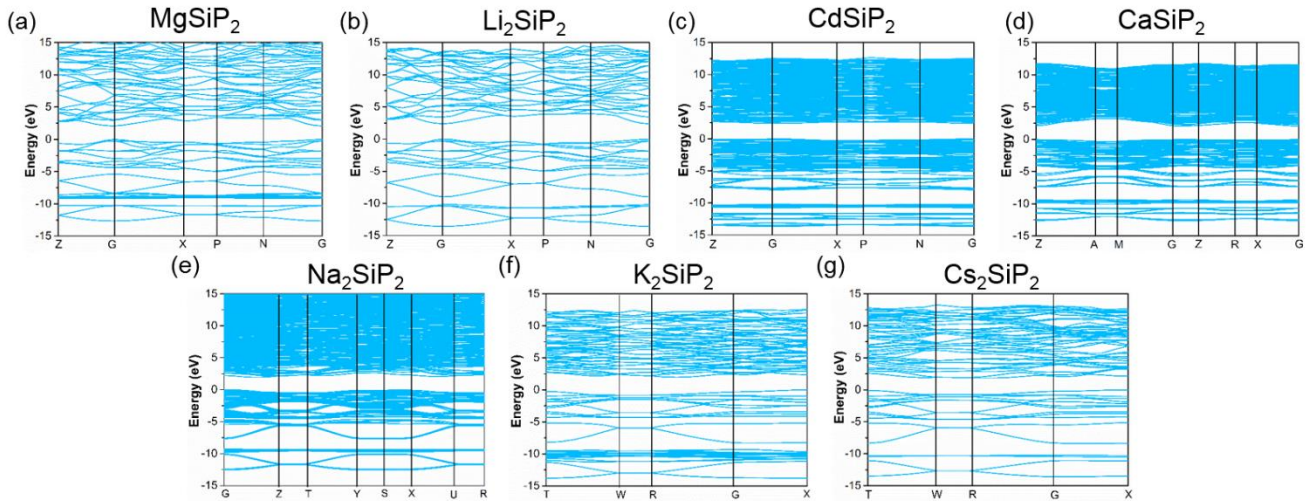


**Figure S4.** 3D ELF isosurfaces at  $\eta = 0.5$  (a), EDD isosurfaces at  $\eta = 1/2 \times \text{maximum}$  (b) and EDD distributions (c) of  $\text{CaSiP}_2$ .

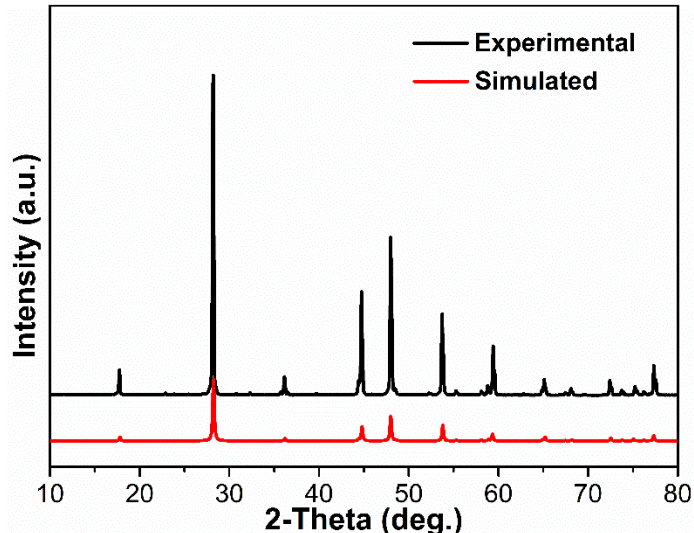
 $\text{Cs}_2\text{SiP}_2$ Figure S5. 3D ELF isosurfaces at  $\eta = 0.5$  (a), EDD isosurfaces at  $\eta = 1/2 \times \text{maximum}$  (b) and EDD distributions (c) of  $\text{Cs}_2\text{SiP}_2$ .Figure S6. 3D ELF isosurfaces at  $\eta = 0.5$  (left column), EDD isosurfaces at  $\eta = 1/2 \times \text{maximum}$  (middle column) and EDD distributions (right column) of  $\text{MgSiAs}_2$  (a, d and g),  $\text{RbSiAs}_2$  (b, e and h),  $\text{SrSiAs}_2$  (c, f and i)

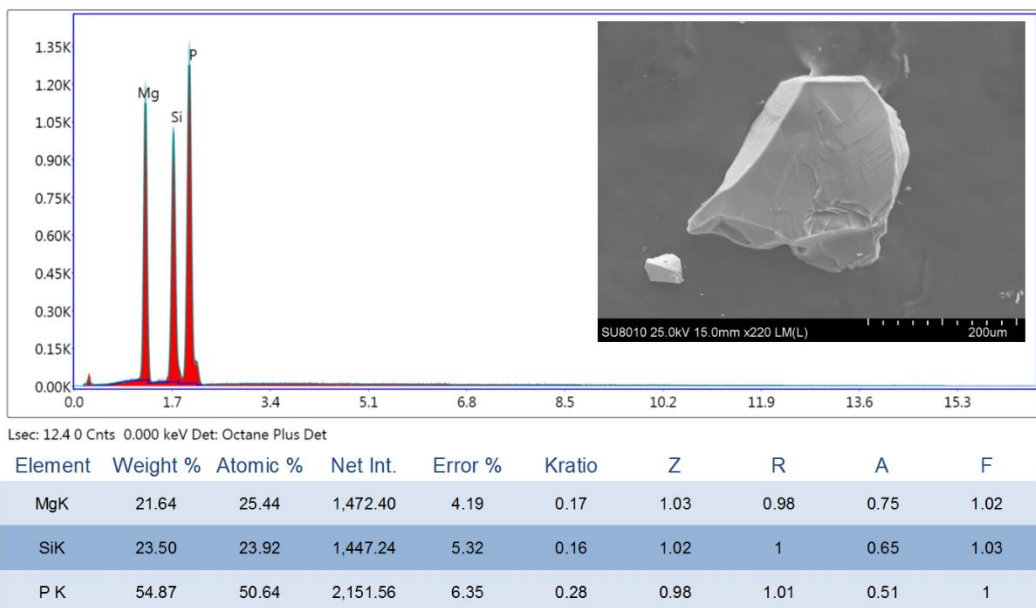
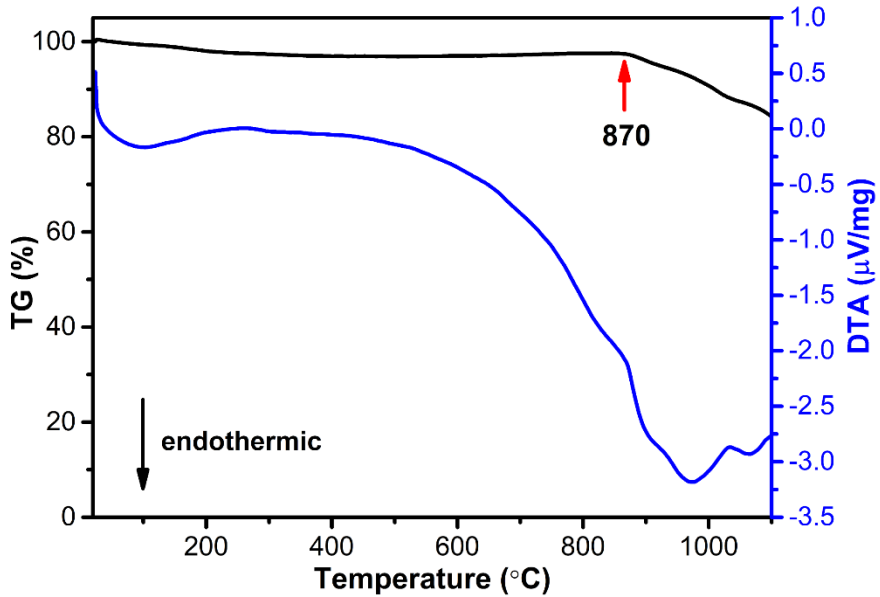


**Figure S7.** CBM structure comparison of MgSiP<sub>2</sub> (a, b) and CaSiP<sub>2</sub> (c, d), Li<sub>2</sub>SiP<sub>2</sub> (e, f) and K<sub>2</sub>SiP<sub>2</sub> (g, h).



**Figure S8.** Band structure of MgSiP<sub>2</sub> (a), Li<sub>2</sub>SiP<sub>2</sub> (b), CdSiP<sub>2</sub> (c), CaSiP<sub>2</sub> (d), Na<sub>2</sub>SiP<sub>2</sub> (e), K<sub>2</sub>SiP<sub>2</sub> (f) and Cs<sub>2</sub>SiP<sub>2</sub> (g).



**Figure S9.** Powder XRD patterns of the experimental and simulated for MgSiP<sub>2</sub>.**Figure S10.** Energy-dispersive X-ray Spectroscopy analysis of MgSiP<sub>2</sub>.**Figure S11.** TG-DTA curves of MgSiP<sub>2</sub>.

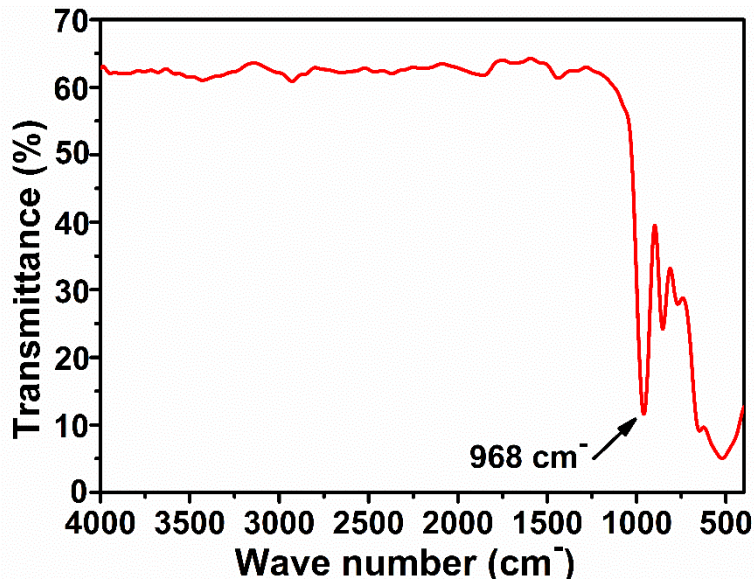


**Figure S12.** IR transmittance spectrum of  $\text{MgSiP}_2$ .

### Reference

1. J. Chen, C. Lin, D. Zhao, M. Luo, G. Peng, B. Li, S. Yang, Y. Sun, N. Ye, *Angew. Chem., Int. Ed.* **2020**, *59*, 23549-23553.
2. A. V. Olenev, O. S. Oleneva, A. V. Shevelkov, B. A. Popovkin, *Russian Chemical Bulletin* **2003**, *52*, 570-575.
3. P. G. Schunemann, K. T. Zawilski, L. A. Pomeranz, D. J. Creeden, P. A. Budni, *J. Opt. Soc. Am. B* **2016**, *33*, D36-43.
4. G. Ambrashevich, G. Babonas, Y. V. Rud, A. Eileika, *Phys. Stat. Sol.* **1981**, *106*, 85-89.
5. A. Roy, U. S. Shenoy, K. Manjunath, P. Vishnoi, U. V. Waghmare, C. N. R. Rao, *J. Phys. Chem. C* **2016**, *120*, 15063-15069.
6. G. Zhang, L. Wei, L. Zhang, X. Wang, B. Liu, X. Zhao, X. Tao, *J. Cryst. Growth* **2017**, *473*, 28-33.
7. I. E. Zanin, K. B. Aleinikova, M. Y. Antipin, *Crystallography Reports* **2003**, *48*, 199-204.
8. J. Chen, C. Lin, F. Xu, S. Yang, Y. Sun, X. Zhao, X. Jiang, B. Li, T. Yan, N. Ye, *Chem. Mater.* **2020**, *32*, 10246-10253.
9. S. Lee, S. L. Carnahan, G. Akopov, P. Yox, L. L. Wang, A. J. Rossini, K. Wu, K. Kovnir, *Adv. Funct. Mater.* **2021**, *31* (16), 2010293.
10. K. Feng, W. Yin, R. He, Z. Lin, S. Jin, J. Yao, P. Fu, Y. Wu, *Dalton Trans* **2012**, *41*, 484-489.
11. S. Zhao, P. Luo, S. Yang, X. Zhou, Z. Wang, C. Li, S. Wang, T. Zhai, X. Tao, *Adv. Opt. Mater.* **2021**, *9*, 2100198.
12. J. Mark, J. Wang, K. Wu, J. G. Lo, S. Lee, K. Kovnir, *J. Am. Chem. Soc.* **2019**, *141*, 11976-11983.
13. K. Feng, L. Kang, W. Yin, W. Hao, Z. Lin, J. Yao, Y. Wu, *J. Solid State Chem.* **2013**, *205*, 129-133.
14. A. Haffner, V. Weippert, D. Johrendt, *Z. Anorg. Allg. Chem.* **2020**, *647*, 326-330.
15. J. Mark, J.-A. Dolyniuk, N. Tran, K. Kovnir, *Z. Anorg. Allg. Chem.* **2019**, *645*, 242-247.
16. J. Chen, C. Lin, G. Peng, F. Xu, M. Luo, S. Yang, S. Shi, Y. Sun, T. Yan, B. Li, N. Ye, *2019*, *31*, 10170-10177.
17. Y. Sun, J. Chen, S. Yang, B. Li, G. Chai, C. Lin, M. Luo, N. Ye, *Adv. Opt. Mater.* **2021**, *9*, 2002176.
18. Y. Sun, C. Lin, J. Chen, F. Xu, S. Yang, B. Li, G. Yang, M. Luo, N. Ye, *Inorg. Chem.* **2021**, *60*, 7553-7560.
19. G. C. Catella, D. Burlage, *MRS Bulletin* **2013**, *23*, 28-36.
20. X. Zhang, J. Yao, W. Yin, Y. Zhu, Y. Wu, C. Chen, *Opt. Express* **2015**, *23*, 552-558.
21. L. I. Isaenko, I. G. Vasilyeva, *J. Cryst. Growth* **2008**, *310*, 1954-1960.
22. K. Kato, V. V. Badikov, L. Wang, V. L. Panyutin, K. V. Mitin, K. Miyata, V. Petrov, *Opt. Lett.* **2020**, *45*, 2136-2139.
23. W. Huang, Z. He, S. Zhu, B. Zhao, B. Chen, S. Zhu, *Inorg. Chem.* **2019**, *58*, 5865-5874.
24. G. D. Boyd, E. Buehler, F. G. Storz, *Appl. Phys. Lett.* **1971**, *18*, 301-304.

25. Q.-T. Xu, Z.-D. Sun, Y. Chi, H.-G. Xue, S.-P. Guo, *J. Mater. Chem. C* **2019**, *7*, 11752-11756.
26. R. Wang, F. Liang, F. Wang, Y. Guo, X. Zhang, Y. Xiao, K. Bu, Z. Lin, J. Yao, T. Zhai, F. Huang, *Angew. Chem., Int. Ed.* **2019**, *58*, 8078-8081.
27. S. P. Guo, Y. Chi, H. G. Xue, *Angew. Chem., Int. Ed.* **2018**, *57*, 11540-11543.
28. R. Ye, X. Cheng, B.-W. Liu, X.-M. Jiang, L.-Q. Yang, S. Deng, G.-C. Guo, *J. Mater. Chem. C* **2020**, *8*, 1244-1247.
29. A. Zhou, C. Lin, B. Li, W. Cheng, Z. Guo, Z. Hou, F. Yuan, G.-L. Chai, *J. Mater. Chem. C* **2020**, *8*, 7947-7955.
30. Y. Guo, F. Liang, J. Yao, Z. Lin, W. Yin, Y. Wu, C. Chen, *Inorg. Chem.* **2018**, *57*, 6795-6798.